U.S. DEPARTMENT OF COMMERCE
National Technical Information Service
PB-299 400

A Kilometer Pathlength Fourier-Transform Infrared System for the Study of Trace Pollutants in Ambient and Synthetic Atmospheres

(U.S.) Environmental Sciences Research Lab, Research Triangle Park, NC

1978

EPA-600/J-78-131
JOURNAL ARTICLE

PB 299400

Reprinted from

ATMOSPHERIC ENVIRONMENT

Vol. 12, *No.* 4, *pp.* 865–875

A KILOMETER PATHLENGTH FOURIER-TRANSFORM INFRARED SYSTEM FOR THE STUDY OF TRACE POLLUTANTS IN AMBIENT AND SYNTHETIC ATMOSPHERES

E. C. TUAZON, R. A. GRAHAM, A. M. WINER, R. R. EASTON, J. N. PITTS, JR and P. L. HANST*

Statewide Air Pollution Research Center, University of California, Riverside, CA 92521, U.S.A.
*Environmental Protection Agency, Research Triangle Park, NC 27711, U.S.A.

REPRODUCED BY
NATIONAL TECHNICAL
INFORMATION SERVICE
U.S. DEPARTMENT OF COMMERCE
SPRINGFIELD, VA. 22161

PERGAMON PRESS
OXFORD · NEW YORK · FRANKFURT · PARIS
1978

TECHNICAL REPORT DATA
(Please read Instructions on the reverse before completing)

1. REPORT NO.	2.	3. RECIPIENT'S ACCESSION NO.
EPA-600/J-78-131	JOURNAL ARTICLE	PB299400

4. TITLE AND SUBTITLE	5. REPORT DATE
A KILOMETER PATHLENGTH FOURIER-TRANSFORM INFRARED SYSTEM FOR THE STUDY OF TRACE POLLUTANTS IN AMBIENT AND SYNTHETIC ATMOSPHERES	6. PERFORMING ORGANIZATION CODE
7. AUTHOR(S) E.C. Tuazon, R.A. Graham, A.M. Winer, R.R. Easton, J. N. Pitts, Jr. and P. L. Hanst*	8. PERFORMING ORGANIZATION REPORT NO.
9. PERFORMING ORGANIZATION NAME AND ADDRESS Environmental Sciences Research Laboratory Office of Research and Development U.S. Environmental Protection Agency Research Triangle Park, North Carolina 27711	10. PROGRAM ELEMENT NO. 1AA603A 11. CONTRACT/GRANT NO.
12. SPONSORING AGENCY NAME AND ADDRESS *Environmental Sciences Research Laboratory-RTP, NC Office of Research and Development U.S. Environmental Protection Agency Research Triangle Park, North Carolina 27711	13. TYPE OF REPORT AND PERIOD COVERED 14. SPONSORING AGENCY CODE EPA/600/09

15. SUPPLEMENTARY NOTES
REFERENCE: Atmos. Environ., 12 (4): 865-875, 1978

16. ABSTRACT

A Fourier-transform infrared system operable at pathlengths up to 2 km has been constructed for the detection and measurement of trace contaminants in the ambient atmosphere and in controlled smog formation studies. The long optical path is achieved by the use of an eight-mirror multiple reflection cell with a 22.5-m base path. The design, construction and use of this novel folded-path optical system are described in detail. In preliminary ambient air measurements at Riverside, California, during the period August-October, 1976, ppb concentrations of formaldehyde, nitric acid, formic acid and ammonia (in addition to O_3 and PAN) were measured in ambient air.

17. KEY WORDS AND DOCUMENT ANALYSIS

a. DESCRIPTORS	b. IDENTIFIERS/OPEN ENDED TERMS	c. COSATI Field/Group
* Air pollution * Infrared spectroscopy * Design * Construction Field tests Test chambers	Fourier-transform infrared system Riverside, California	13B 14B

18. DISTRIBUTION STATEMENT	19. SECURITY CLASS (This Report)	21. NO. OF PAGES
RELEASE TO PUBLIC	UNCLASSIFIED	14
	20. SECURITY CLASS (This page) UNCLASSIFIED	22. PRICE A02-A01

EPA Form 2220-1 (9-73)

Atmospheric Environment Vol. 12, pp. 865–875
Pergamon Press Ltd. 1978. Printed in Great Britain.

0004-6981/78/0401-0865$02.00/0

A KILOMETER PATHLENGTH FOURIER-TRANSFORM INFRARED SYSTEM FOR THE STUDY OF TRACE POLLUTANTS IN AMBIENT AND SYNTHETIC ATMOSPHERES

E. C. TUAZON, R. A. GRAHAM, A. M. WINER, R. R. EASTON and J. N. PITTS, JR*

Statewide Air Pollution Research Center, University of California, Riverside, CA 92521, U.S.A.

and

P. L. HANST

Environmental Protection Agency, Research Triangle Park, NC 27711, U.S.A.

(*First received* 28 *March* 1977 *and in final form* 1 *July* 1977)

Abstract—A Fourier-transform infrared (FT–i.r.) system operable at pathlengths up to 2 km has been constructed for the detection and measurement of trace contaminants in the ambient atmosphere and in controlled smog formation studies. The long optical path is achieved by the use of an eight-mirror multiple reflection cell with a 22.5-m base path. The design, construction and use of this novel folded-path optical system are described in detail. In preliminary ambient air measurements at Riverside, California, during the period August–October, 1976, ppb concentrations of formaldehyde, nitric acid, formic acid and ammonia (in addition to O_3 and PAN) were measured in ambient air.

INTRODUCTION

For the past 25 years long-path infrared (LP-i.r.) absorption spectroscopy has played an important role in the identification and quantitative determination of trace pollutants in both ambient air and synthetic smog systems. Among the most significant contributions made with this technique were the first spectroscopic proof of ozone formation in photochemical smog in 1956 (Stephens *et al.*, 1956a) and the discovery of the highly toxic secondary pollutant peroxyacetyl nitrate (PAN) (Stephens *et al.*, 1956a; Stephens *et al.*, 1956b; Stephens *et al.*, 1959), a compound unknown to chemists prior to its characterization in photochemical smog by LP-i.r. spectroscopy in 1956. These results were obtained with prism i.r. spectrophotometers and White-type multiple reflection cells (White, 1942) at pathlengths of 40–400 m.

Other important early applications of this method included studies of irradiated auto exhaust (Stephens and Schuck, 1958), plant damage (Darley *et al.*, 1959), hydrocarbon reactivity (Stephens and Scott, 1962; Heuss and Glasson, 1968) and ozone–olefin reactions (Hanst *et al.*, 1958). More recent applications of the LP-i.r. method include investigations of ozone–olefin (McAfee *et al.*, 1974; McNelis, 1974; Niki *et al.*, 1975) and sulfur dioxide (Daubendiek and Calvert, 1975) systems as well as studies of the composition of polluted urban air (Hanst *et al.*, 1975a), halogenated pollutants and other atmospheric trace gases (Hanst *et al.*, 1975b), oxidation of chlorinated ethylenes (Gay *et al.*, 1976), nitrous acid equilibria (Chan *et al.*, 1976) and calibration techniques for ozone (Kopczynski and Bufalini, 1971; Pitts *et al.*, 1976; McAfee *et al.*, 1976).

The LP-i.r. technique is often employed in a complementary fashion with gas chromatography (GC) and combined GC–MS, which are more sensitive for specific hydrocarbon analysis. Infrared detection, on the other hand, by virtue of its specificity and *in-situ*, non-destructive and quantitative nature, is particularly useful in the measurement of organic oxygenates and nitrogenous compounds, including labile species, as well as a variety of organic products. In recent years the evolution and application of the LP-i.r. method has proceeded on two fronts (Hanst, 1971; Hanst *et al.*, 1973): first, the development of more sophisticated multiple reflection systems of greater total pathlengths, and second, the replacement of dispersive (i.e. prism and grating) i.r. spectrophotometers by Michelson interferometers equipped with minicomputers for carrying out fast Fourier transforms of the resulting interferograms. The latter development has added high spectral resolution (i.e. 0.06–1.0 cm^{-1}) and good time-resolution to the strengths of the LP-i.r. method cited above.

The background for our present research program was an investigation conducted by Hanst and coworkers (1975a) in Pasadena, California, during November, 1972, and July–August, 1973. In this program, a Digilab Fourier-Transform Spectrometer (FTS) and a folded-path optical system with a base path of 8.7 m and a maximum pathlength of 417 m (enclosed in a glass tube 9.1 m long and 0.3 m dia) were employed on the roof of the Keck Engineering Building at the California Institute of Technology. In

* Author to whom correspondence should be addressed.

this study formic acid was observed spectroscopically in ambient air for the first time, at concentrations as high as 70 ppb, and low upper limits were set for the presence of HNO_3, N_2O_5 and alkyl nitrates ($\leq$10 ppb) and for formaldehyde ($\leq$30 ppb). The Pasadena study was viewed as a prelude to a more extensive research program consisting of systematic studies, at several sites, in which (a) the LP-i.r. experiments would be augmented by a full range of supplementary analytical methods, and (b) the detection limits of the LP-i.r. method would be extended to still lower concentration regimes. Consequently, a new LP-i.r. spectrometer system, which offers the possibility of fulfilling these research objectives, was developed at Environmental Protection Agency Laboratories and then modified and set up for field studies at the Statewide Air Pollution Research Center on the University of California, Riverside campus. The system consists of a Digilab FTS-14 spectrometer with data system and peripherals and a 22.5 m base-path, multi-pass optical system capable of total pathlengths as long as 2 km. In this paper we report the design, properties and siting of this system and its preliminary applications to ambient air studies in the fall of 1976.

KILOMETER PATHLENGTH MULTIPLE REFLECTION CELL AND FOURIER-TRANSFORM i.r. SYSTEM

Figure 1 depicts the multiple reflection cell and FT–i.r. spectrometer. Four rectangular mirrors, cut from a single 41 cm dia. Pyrex blank, comprise the in-focus end (nesting mirrors) of the cell. Three of these mirrors are 6.4 cm wide and 32 cm long, while the fourth is slightly shorter (28 cm) to provide the entrance and exit apertures for the infrared beam. The out-of-focus optical assembly (collecting mirrors) consists of four 30 cm dia. mirrors and is 22.5 m (the average radius of curvature of the eight mirrors) from the nesting mirror assembly. All mirrors are optically polished and gold-coated for maximum reflectivity in the i.r.

The cell housing consists of a sectional rectangular aluminum frame (total dimensions: 0.81 × 0.84 × 23 m) enclosed at the bottom and one side with Plexiglas and with 50 μm FEP Teflon on the other two faces. Teflon was used for the two sides most exposed to the sun to provide good transmission of solar radiation when the cell is being used as a reaction chamber for synthetic systems. A removable sun screen can be installed (not shown in Fig. 1) over the entire length of the cell to reduce thermal effects on the stability of the i.r. beam during ambient monitoring. To minimize vibrations, the mirror assemblies are each mounted on platforms completely independent of the cell housing.

Coupled with the cell is a Digilab interferometer system housed in a 3.7 × 3.7 m air-conditioned building. The collimated i.r. beam from a Nernst glower is modulated by a Digilab Model 296 Michelson IR interferometer capable of spectral resolutions as high as 0.5 cm^{-1} and is imaged at the entrance aperture of the cell. The beam exiting from the cell is sent to either of two liquid-N_2 cooled detectors: a photovoltaic InSb detector for the 2000–3900 cm^{-1} range or a photoconductive HgCdTe detector for the 600–2000 cm^{-1} region. Data collection and processing are performed by a Data General Nova 1200 computer with 4096 16-bit words of core. A disk unit (128 K-words) is used for software storage and partial

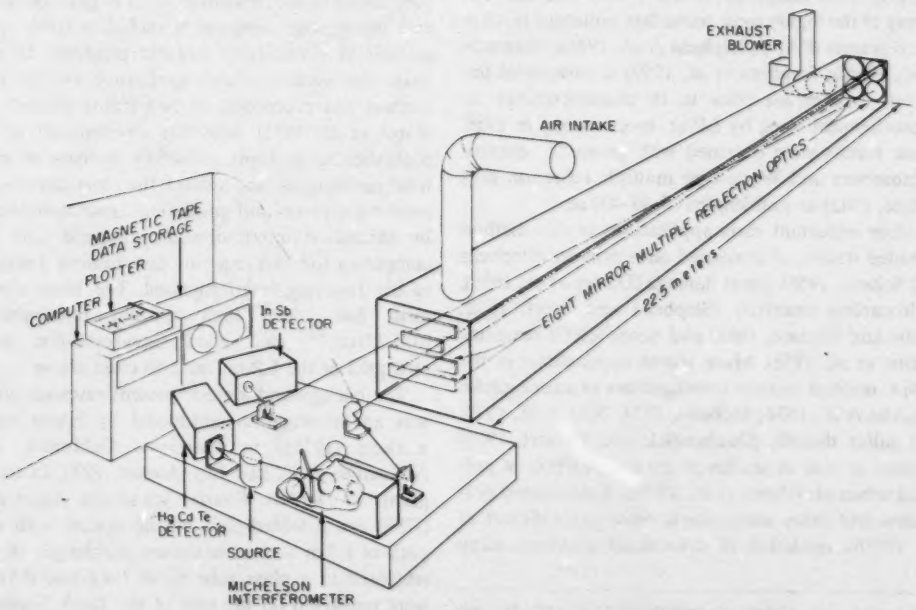

Fig. 1. Km pathlength FT-i.r. system.

storage of data. Archival data storage of both raw interferograms and computed spectra is provided by a Kennedy Model 9700 magnetic tape unit. The Digilab system is also equipped with a Houston Instruments pen plotter, an oscilloscope and a teletype.

The instrumentation was set up on the roof of the Webber Hall East building on the U.C. Riverside campus. This location is 24 m above the ground and provides unobstructed exposure to prevailing winds from the west, north or south. No ventilation ducts or exhaust blowers are located on this roof. During ambient monitoring, atmospheric sample is drawn continuously through the cell at a rate of $330\,l\,s^{-1}$ (one cell volume every 50 s) by a 1/4 hp blower at one end. Air enters the other end of the cell through a 36 cm dia pipe with an intake 2 m above the roof.

Optical alignment and multiple reflection cell operation

The design of the eight-mirror cell employed in this study, as well as those of similar multiple-mirror cells, has been described in detail by Hanst (1971). The operation of the eight-mirror cell is briefly described below with reference to Fig. 2.

The incoming beam of light is imaged at the entrance aperture, designated I, at the nesting mirror assembly. The beam diverges from I to fill mirror C1 and is refocused onto N1. The beam is then directed to C2→N2→C3→N3→C4 and finally to the exit aperture 0 during one complete pass through the cell's optics. For a second pass, the exiting beam at 0 is re-imaged on N4 and the above sequence of reflections is repeated. The sequence by which the i.r. beam is reflected by the individual mirrors is illustrated by numbered dots in Fig. 2 for six complete passes through the cell. Six images on each of the nesting mirrors (N1, N2, and N3) are thus equivalent to a pathlength of $6 \times 8 \times 22.5 = 1080$ m (~ 1 km) in the present configuration.

The transfer optics between the interferometer and the cell (Fig. 1) focuses a magnified image (2.5×6.4 cm) of the source element at the entrance aperture. Since a laser beam provides the most direct visual check of alignment, a 4 mW He–Ne laser was interposed in the transfer optics and made coincident with the center of the i.r. beam. This was accomplished with the visible component of the glower source transmitted by a quartz beamsplitter instead of the KBr–Ge beamsplitter normally used for i.r. work. The laser can be removed when recording interferograms and re-installed reproducibly during alignment checks. Stray radiation in the beam leaving the cell, which results from the primary beam overfilling mirror C1 and striking mirrors C2 and C3, was eliminated by masking a small portion of the beam at the interferometer output. A simple test which determines whether this source of stray radiation is excluded consists of achieving zero signal by detuning mirror C4 with its vertical adjustment.

Temperature variations during the course of a day's experiments were found to cause changes in the optical mounts significant enough to displace the critical settings of the mirrors. The preliminary alignment of the cell optics is carried out by observing that the laser dots are properly centered on the collecting and nesting mirrors. The output at a given pathlength is maximized through the horizontal and vertical adjustments of mirrors C4 and N4. This is accomplished by monitoring the AC signal generated by a chopper installed between the interferometer and transfer optics. A two-position mirror permits alternate data collection on the HgCdTe and InSb detectors. The final criterion of proper alignment is the peak-to-peak height of the interferogram, which represents the total transmitted energy that has been modulated by the interferometer.

Routine data collection was carried out at a pathlength of 1.08 km. The transition between rows of images is still well-defined at this pathlength and can

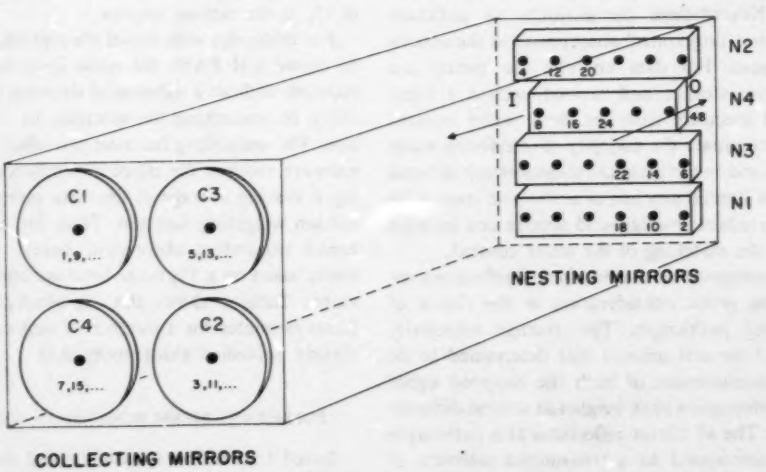

Fig. 2. Eight-mirror multiple reflection system. (Numbered dots indicate sequence of reflections during six complete passes through the cell; I = entrance aperture; O = exit aperture.)

be monitored precisely with the alignment procedure described. The system has been operated at a pathlength of 2 km, on some occasions, with a substantial decrease in total signal. At these longer pathlengths, partial overlapping of the images at the exit aperture necessitates a careful calibration procedure (using the known absorptivity of an appropriate gas) to determine the effective pathlength attained.

Data collection and signal-to-noise considerations

During a scan of the interferometer mirror, an audio-frequency sinusoid is generated for each i.r. frequency element. The interferogram is the summation of all such sinusoids from the whole range of incident optical frequencies and is related to the actual spectrum (radiation intensity vs wavelength) by the Fourier-transform. Forty such interferograms were usually co-added to enhance the signal-to-noise ratio in the interferogram, and thus in the computed spectrum. The spectral resolution routinely employed was $0.5\,cm^{-1}$ with 16384 digitized points in each interferogram. At this resolution the vibration–rotation structure of most light molecules present in the atmospheric sample can be resolved and used for positive identification. Data collection with 40 scans, transform computation, routine plotting of a portion of the spectrum and magnetic tape storage could be accomplished within 10 min for each detector. Hence, a time resolution of three complete spectra ($600–4000\,cm^{-1}$) per hour is available to characterize moving smog fronts.

Strong absorptions due to the H_2O and CO_2 content of the atmosphere render certain regions of the infrared unsuitable for detection of pollutant molecules. At pathlengths of 1 km and longer, the spectral windows for i.r. detection are generally limited to the 760–1300, 2000–2230 and $2390–3000\,cm^{-1}$ regions. This means that some characteristic functional group absorptions, such as those due to stretches of the C=O, C=C and OH bonds, generally cannot be employed. Nevertheless, the majority of pollutant molecules have 'fingerprint' absorptions in the accessible i.r. regions. For data analysis the spectra are retrieved from storage and ratioed against a clean background spectrum with the same water content in order to eliminate the majority of interfering water absorptions and to facilitate the measurement of band intensities. A limited amount of arithmetic manipulation of the available background spectra can be used to improve the matching of the water content.

Signal attenuation as the number of reflections increases is the prime consideration in the choice of the operating pathlength. The average reflectivity coefficient of the cell mirrors was determined to be ~0.98 by measurement of both the chopped signal and the interferogram peak heights at several different pathlengths. The 47 mirror reflections at a pathlength of 1080 m correspond to a transmitted intensity of 0.39 times the incident radiation. This value is slightly greater than 1/e (0.37), which has been established as the criterion for maximizing the signal-to-noise ratio for i.r. systems that are detector noise limited (Stephens, 1958, 1961).

To obtain a measure of the best performance of the system, experiments were conducted at night (when thermal effects and vibrations were minimal) and with the cell purged to low relative humidities with dry nitrogen gas. At pathlengths near 1 km, a signal-to-noise level of 400 was attained in the ratio plot. This corresponds to a signal-to-noise level of approx 1000 for a single mirror reflection. From the analysis of Hanst *et al.* (1973) a theoretical detection sensitivity of 0.8 ppb was calculated for a compound which has an absorptivity of $30\,cm^{-1}\,atm^{-1}$ (e.g. PAN). In practice, the theoretical detection sensitivity is not usually achieved due to effects such as building vibrations, concentration fluctuations with time, interfering absorptions and variations in the refractive index of air caused by temperature gradients in the cell.

During the ambient air monitoring experiments, the peak-to-peak signal-to-noise level in the ratioed spectra which could routinely be achieved for regions clear of atmospheric absorptions was 0.5% ($S/N \approx 200$). Theoretically, the noise level can be improved by co-adding more interferograms. The variability of the concentrations of many species in the atmospheric sample, however, limits the amount of signal-to-noise improvement obtainable by longer averaging times.

For many regions, the apparent noise level is increased by spurious difference peaks which arise from non-exact cancellation of background absorptions and small wavenumber shifts between background and sample spectra. The small wavenumber shifts cause finite resolution errors and have their origins in instrumental instability and spatial vignetting of the i.r. beam (Hirschfeld, 1976a, b). Even with good matching of H_2O lines, the peak-to-peak noise is generally about 1% in the ratioed spectra for these regions. Hence, we prefer to establish our operational detection limits on the basis of a signal amplitude of 1% in the ratioed spectra.

For molecules with broad absorption features (such as ozone and PAN) the noise level can usually be reduced, without a substantial decrease in the absorptivity, by smoothing the spectrum to a lower resolution. The smoothing function provided in the Digilab software reduces the effective resolution by calculating a moving average of the data points with a Lorentzian weighting function. Thus, for molecules with broad featureless absorption bands, the detection limits based on a 1% noise level are conservative estimates. Table 1 shows the 1% absorption detection limits estimated for a number of molecules from previously published absorptivity data.

POLLUTANT MEASUREMENTS IN AMBIENT AIR

Initial tests of the system focused on species such as ozone and PAN which occur in substantial concentrations in photochemical air pollution. Ozone

Table 1. Calculated detection limits for several important species using 1 km FT-i.r. system

Compound	Measurement frequency (cm^{-1})	Approximate absorptivities* at 0.5 cm^{-1} spectral resolution (cm^{-1} atm^{-1}, RTP†)	References	Detection limit‡ for present system (ppb)
NH_3	931	48	(Hanst *et al.*, 1975a)	2
	967.5	69		2
HCHO	2779 / 2781.5	25	(Hanst *et al.*, 1975a)	4
HCOOH	1105.3	27§	(Hanst *et al.*, 1975a)	4
HNO_3	896	28	(Hanst *et al.*, 1975a)	4
HONO	853 (*cis*)	71	(Chan *et al.*, 1976)	4¶
N_2O_5	740	40	(Hanst *et al.*, 1975a)	2
	1248	37	(Graham, 1975)	2
O_3	1055	9.7	(Pitts *et al.*, 1976) (McAfee *et al.*, 1976)	10
PAN	793	24	(Stephens, 1964)	4
	1162	32		3
CH_x	2970	4.0	(Hanst *et al.*, 1975a)	23

* $\alpha = \ln(I_0/I)/pl$; Except for HONO, values given for the sharp Q-branches were estimated from absorptivities at 2 cm^{-1} resolution by Hanst *et al.* (1975a). The latter values were multiplied by the ratio of peak height obtained at 0.5 cm^{-1} resolution to that generated by a smoothed plot with an effective resolution of 2 cm^{-1}.

† ~23°C, 760 Torr.

‡ Calculated on the basis of a signal amplitude equal to 1% in the ratioed spectrum.

§ Height of Q-branch only.

¶ Detection limit for total nitrous acid since [t-HONO/c-HONO] ≃ 2.3 at 23°C (Chan *et al.*, 1976).

was useful because it could be conveniently monitored in the cell by a Dasibi continuous analyser which had been independently calibrated, by means of a transfer standard, against a 1 m u.v. spectrophotometer (California Air Resources Board, 1975). FT-i.r. measurements of ozone concentrations were made from the R-branch absorption at 1055 cm^{-1} using the recently determined (Pitts *et al.*, 1976; McAfee *et al.*, 1976) absorptivity (base e) of 9.74 cm^{-1} atm^{-1} (9.74 × 10^{-4} ppm^{-1} m^{-1}). Results from simultaneous measurements of ambient ozone concentrations (in the 50–300 ppb range) by the two methods on October 4–6 are plotted in Fig. 3. The FT-i.r. measurements averaged 0.9% higher than the averaged Dasibi readings for the same time period, and the S.D. of the percentage differences was 4%. Thus, excellent agreement was obtained between the two measurement methods.

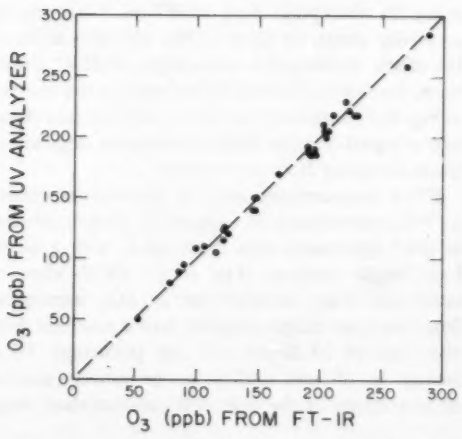

Fig. 3. Comparison of FT-i.r. and u.v.-analyser measurements of ambient ozone concentrations.

Figure 4(a) shows a smoothed plot of a spectrum recorded with the mercury–cadmium telluride detector on October 5, 1976 at 4.34 p.m. ratioed against a spectrum recorded on October 1, 1976 at 11.29 a.m. Bands due to 285 ppb ozone, 15 ppb PAN and 21 ppb NH_3 are marked in the figure. The spurious negative peak at 1125 cm^{-1} is believed to arise from the transformation of a frequency intermittently introduced into the interferogram by the detector preamplifier. The spectrum of Fig. 4(a) was recorded at 0.5 cm^{-1} resolution, but smooth-plotted to an apparent resolution of 2 cm^{-1} to reduce the noise level of the spectrum.

Figure 4(b) is a smoothed spectrum showing the C–H stretching absorptions of methane and other paraffinic hydrocarbons (CH_x). This spectrum was recorded with the indium antimonide detector on October 5, 1976 at 5.43 p.m. and has been smoothed from 0.5 to 2 cm^{-1} since the bands in this spectrum are all broad. The reference spectrum in this case was selected from a series of background spectra obtained by purging the cell with three volumes of high-purity nitrogen gas and adding incremental amounts of water. Use of this nitrogen background permits obser-

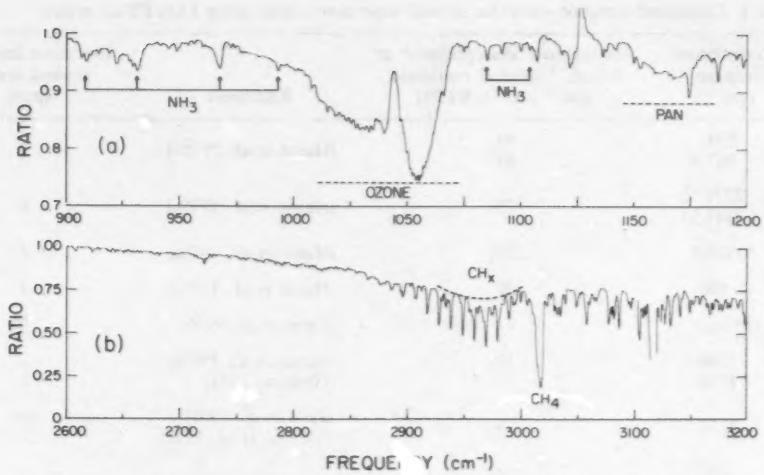

Fig. 4. Riverside ambient air spectra at 2 cm^{-1} spectral resolution, 1080 m pathlength. (a) October 5, 1976 at 4.34 p.m.: 285 ppb O_3, 15 ppb PAN, 21 ppb NH_3 (HgCdTe detector). (b) October 4, 1976 at 5.43 p.m.: 800 ppb CH_x (InSb detector).

vation of both the natural background level of methane (1.5 ppm) and the contribution from anthropogenic sources and indicates a total methane concentration of 2.3 ppm. A total non-methane paraffinic carbon count of 800 ppb is indicated by the strength of the C–H band envelope at 2970 cm^{-1}. This value agrees with that measured concurrently with a Beckman 6800 gas chromatograph.

Ammonia

A species of special interest in preliminary measurements at the Riverside site (i.e. at the eastern or 'downwind' end of the California South Coast Air Basin) was ammonia (NH_3), a primary pollutant. Originating primarily upwind of Riverside from agricultural and industrial sources, NH_3 plays an important role in the stabilization of nitric acid as ammonium nitrate aerosol. High levels of particulate nitrates (e.g. 24-h average concentrations as high as 70 $\mu g\ m^{-3}$) have been measured at the eastern end of the South Coast Air Basin (Grosjean *et al.*, 1976) and characterization of sources and ambient concentrations of NH_3 are important in understanding mechanisms of gas-to-particle conversion. Semi-continuous methods for the analysis of ppb concentration of NH_3 have only recently been proposed (Farber and Rossano, 1975); hence, quantitative determination of NH_3 in the 2–20 ppb concentration range with the FT–i.r. facility is of interest.

The portions of the i.r. spectrum of ammonia which cover its most useful analytical wavelengths are shown in Fig. 5(a). Although all of the absorption features in the figure are due to ammonia, the most useful features for identification purposes are the strong inversion doublet bands at 931 and 967 cm^{-1}. The spectrum shown was recorded for an NH_3 sample injected into the cell and corresponds to a concentration of 135 ppb. A detection limit of ~2 ppb has been calculated for NH_3. Reference spectra generated in this manner can be easily retrieved from storage and provide a line-by-line comparison when superimposed on sample spectra being analysed.

Figures 6(a) and 6(b) are spectra from ambient air monitoring runs on a clear and sunny day (October 1, 1976). The top spectrum (a) is a single beam scan taken at 11.29 a.m., and the middle spectrum (b) was recorded at 12.48 p.m. During this interval of time winds from the west became noticeably stronger. Several weak absorptions in the middle spectrum, which are interspersed with the stronger atmospheric H_2O absorption lines, are not present in the top spectrum. The ratio plot of the two single-beam runs, presented in Fig. 6(c), gives a clear presentation of the characteristic vibration–rotation lines of NH_3. An ambient air concentration of ~32 ppb was calculated using the absorption peak at 967 cm^{-1} and the absorptivity shown in Table 1. Fig. 6(c) also illustrates the effects of non-exact cancellation of H_2O absorptions. Spurious difference spikes such as the one seen in Fig. 6(c) (marked ×) are often observed (see discussion of signal-to-noise above) and can be large at positions of strong H_2O absorptions.

FT-i.r. measurements made in this study of ambient air NH_3 concentrations between 25 and 50 ppb were in good agreement with those made with a nearby Lear–Siegler analyser (Fitz *et al.*, 1976) when the latter data were corrected for an SO_2 interference. Since the Lear–Siegler analyser had a practical detection limit of 10–20 ppb, the km pathlength FT-i.r. facility is of real utility in permitting accurate measurements in the low ppb concentration range.

Formaldehyde

A search for the absorption features of formalde-

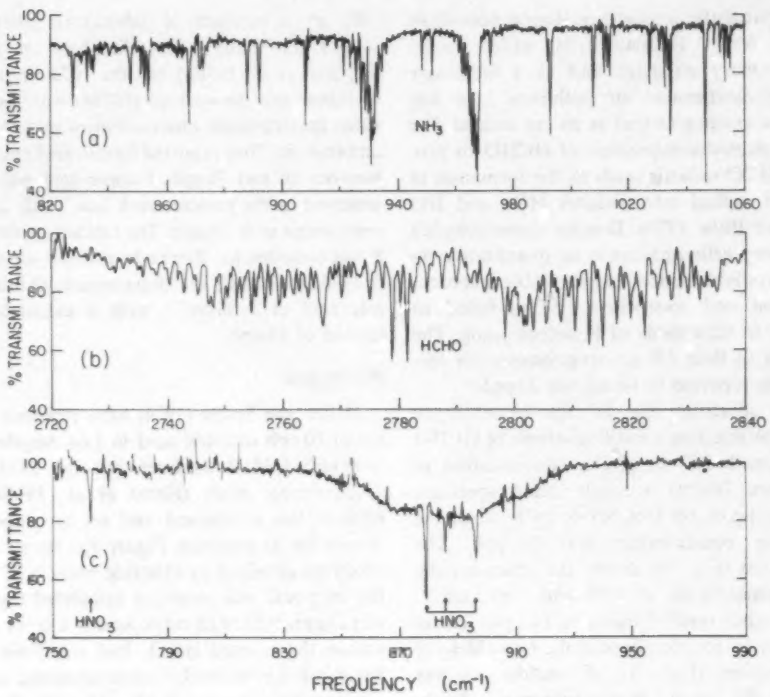

Fig. 5. Reference spectra with 0.5 cm^{-1} spectral resolution, 1080 m pathlength. (a) Ammonia, 135 ppb. (b) Formaldehyde, 160 ppb. (c) Nitric acid, 127 ppb.

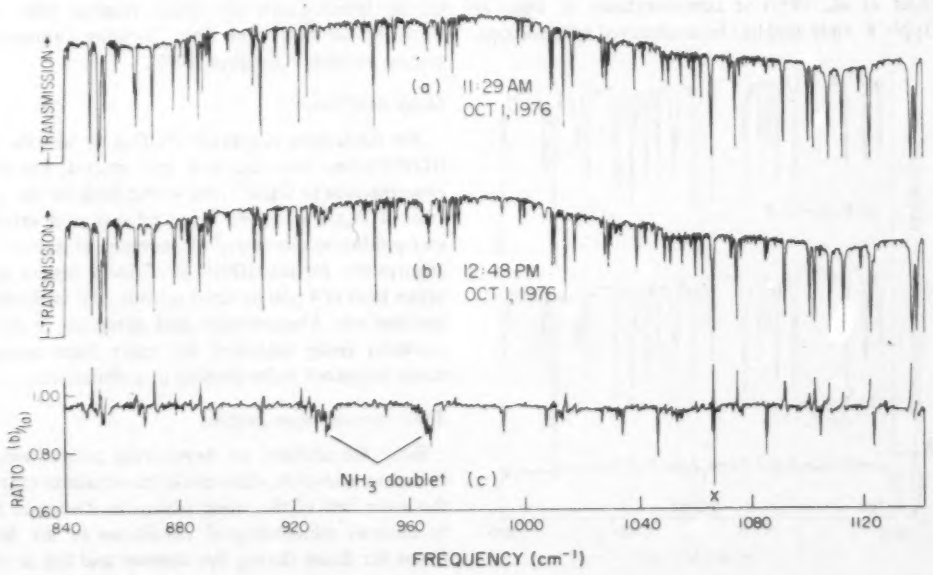

Fig. 6. Riverside ambient air spectra at 0.5 cm^{-1} spectral resolution, 1080 m pathlength. NH_3 concentration, 32 ppb.

hyde was of particular importance during periods of high oxidant levels. Formaldehyde, which occurs both as a primary pollutant and as a secondary product in photochemical air pollution, is a key photo-initiator in smog as well as an eye irritant. For example, the photodecomposition of HCHO to produce H and HCO radicals leads to the formation of the important radical intermediates HO_2 and HO (Finlayson and Pitts, 1976). Despite formaldehyde's importance, very little qualitative or quantitative information is available concerning its ambient concentrations. Hanst and co-workers (1975a) failed to detect HCHO in their study of Pasadena smog. The detection limit of their LP–i.r. spectrometer for formaldehyde was reported to be approx 30 ppb.

A reference spectrum (Fig. 5b) for formaldehyde was obtained by injecting a purified sample of HCHO into the long-path cell to give a concentration of 160 ppb. Figure 7(b) is a single beam spectrum recorded at 5.11 p.m. on October 6, 1976, when the ambient ozone concentration was 210 ppb. The ratioed spectrum (Fig. 7c) shows the characteristic doublet of formaldehyde at 2779 and 2781.5 cm^{-1}. Many of the other small features in the plot correspond to vibration–rotation lines in the formaldehyde reference spectrum (Fig. 5b). Formaldehyde was present during this run at a concentration of ~8 ppb. The detection limit of the FT-i.r. system for formaldehyde using the doublet at 2780 cm^{-1} has been calculated to be ~4 ppb using the absorptivity shown in Table 1.

Formic acid

The detection of formic acid in Los Angeles air by a wet chemical method was reported in 1955 (Mader *et al.*, 1955) at concentrations as high as 410 ppb. Formic acid has been observed spectroscopically as a product of laboratory photooxidation studies for many years (Stephens *et al.*, 1956a; Stephens *et al.*, 1956b), but the 1973 Pasadena study of Hanst and co-workers (1975a) was the only previous spectroscopic observation of this compound in ambient air. They reported formic acid concentrations between 10 and 70 ppb. Formic acid was frequently observed in the present work (see Table 2) with concentrations of 4–19 ppb. The ratioed spectrum in Fig. 8 was recorded for Riverside ambient air on October 5, 1976, and shows the characteristic *Q*-branch of formic acid at 1105 cm^{-1} with a calculated concentration of 19 ppb.

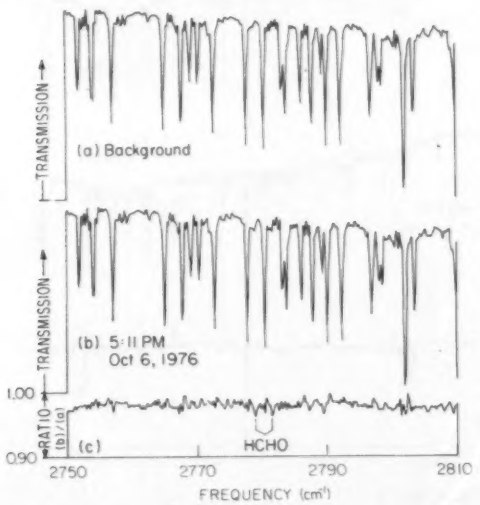

Fig. 7. Riverside ambient air spectra at 0.5 cm^{-1} spectral resolution, 1080 m pathlength. Formaldehyde concentration, 8 ppb.

Nitric acid

Miller and Spicer (1974) have reported measuring up to 10 ppb of nitric acid in Los Angeles air using a modified Mast analyser, but the 1973 Pasadena spectroscopic study (Hanst *et al.*, 1975a) did not observe this compound and set an upper limit of 10 ppb for its presence. Figure 5(c) shows a reference spectrum obtained by injecting nitric acid vapor into the long-path cell to give a calculated concentration of 127 ppb. Although nitric acid is a fairly stable substance, the injected HNO_3 had a half-life of only a few minutes in our cell. A small ammonia background concentration (8 ppb) in the cell with the acid also disappeared rapidly.

An ambient air spectrum taken on October 5 at 7.22 p.m. is shown in Fig. 9(b). The ratioed spectrum (Fig. 9c) indicates the presence of 6 ppb of nitric acid. In spectra taken during the smog episodes of October 5 and 6, the nitric acid spectral features disappear when the ammonia level rises. This supports the view that the high levels of ammonia in the eastern end of the South Coast Air Basin remove nitric acid through chemical reaction, forming ammonium nitrate aerosols (Grosjean, 1977).

Other compounds

No dinitrogen pentoxide (N_2O_5) or nitrous acid (HONO) has been found in our spectra. From the absorptivities in Table 1, the upper limit for the presence of N_2O_5 is 2 ppb. Since nitrous acid exists as an equilibrium mixture of its geometrical isomers, the absorptivity for *cis*-HONO in Table 1 results in an upper limit of 4 ppb for total nitrous acid in Riverside ambient air. Absorptivities and detection limits are currently being evaluated for other trace contaminants suspected to be present in polluted air.

Time–concentration profiles

Since the ambient air monitoring project was initiated in mid-1976, data could be obtained only for the latter half of the smog season in Riverside. Due to unusual meteorological conditions in the South Coast Air Basin during the summer and fall of 1976, no severe smog episodes were observed during the period of study. Most of the data presented in the previous sections were obtained on October 4, 5 and

Table 2. Pollutant concentrations (ppb) in Riverside air*

Date	Time	O_3	NH_3	PAN	HCOOH	HCHO†	HNO_3
Oct. 4	1033	52	6	5	—	—	—
	1208	85	5	4	—	—	—
	1252	89	3	4	—	—	—
	1511	113	31	5	—	—	—
	1603	145	24	7	5	—	—
	1700	228	18	18	7	4	—
	1730	220	4	14	9	9	—
	1759	213	—	14	14	8	—
	1827	203	—	13	11	—	—
	1903	106	—	8	4	—	—
	1913	78	—	5	5	—	—
Oct. 5	1552	140	36	4	—	4	—
	1634	285	21	15	5	10	—
	1705	258	15	15	7	8	—
	1736	218	20	12	9	10	—
	1805	210	14	12	7	7	—
	1833	205	—	13	19	9	4
	1922	150	—	10	13	7	6
	1947	123	—	9	8	—	4
Oct. 6	1142	150	4	11	14	—	6
	1155	170	4	11	13	—	4
	1258	120	14	11	—	—	5
	1320	115	23	3	—	—	4
	1429	185	43	6	—	—	4
	1514	218	31	3	8	4	—
	1556	190	22	12	4	—	—
	1630	187	21	9	5	4	—
	1658	200	30	9	8	8	—
	1725	192	25	9	6	6	—
	1753	185	26	9	6	8	—
	1833	125	12	7	5	—	—
	1853	108	3	7	6	—	—

* Dashes indicate below detection limit.
† Formaldehyde measurements were made with the InSb detector approximately 10 min after the times listed in the table for the HgCdTe detector spectra.

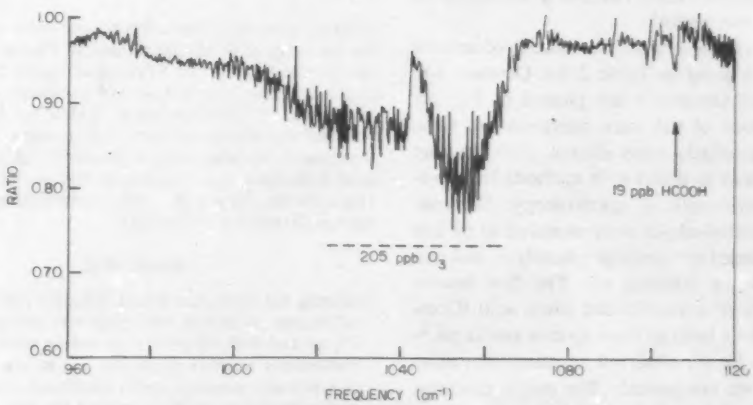

Fig. 8. Riverside ambient air spectrum (October 5, 1976 at 6.33 p.m.) at 0.5 cm^{-1} spectral resolution, 1080 m pathlength. Formic acid, 19 ppb; ozone, 205 ppb.

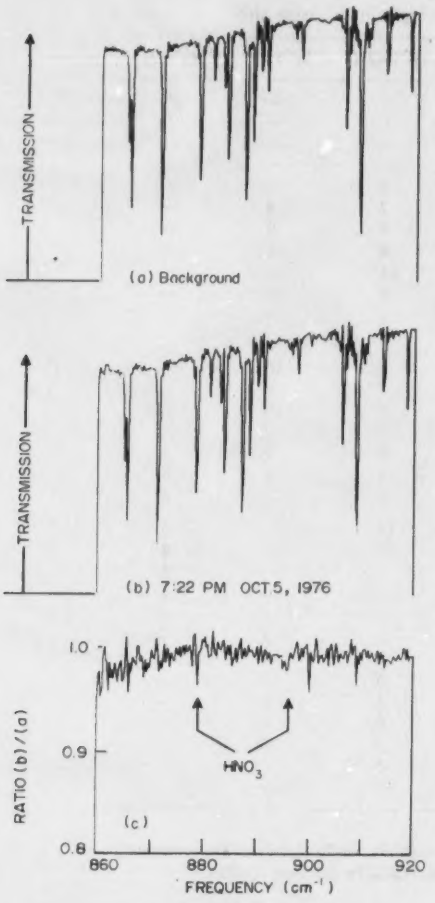

Fig. 9. Riverside ambient air spectrum (October 5, 1976 at 7.22 p.m.) at 0.5 cm^{-1} spectral resolution, 1080 m pathlength. Nitric acid concentration, 6 ppb.

6. The ozone concentration reached a maximum of 285 ppb during this period.

Time–concentration data for the species of interest in this study are given in Table 2 for October 4–6, and the data for October 6 are plotted in Fig. 10. The concentrations of the trace contaminants nitric acid and formaldehyde were always ≤ 10 ppb and would thus be hard to detect with methods less sensitive than km pathlength i.r. spectroscopy. The concentrations of formaldehyde were expected to be low since this compound can undergo photolysis and oxidation reactions in polluted air. The fast heterogeneous reaction of ammonia and nitric acid (Grosjean, 1977) removes both of these species and is probably responsible for the observed negative correlation between these two compounds. The major products, PAN and formic acid, are fairly stable and accumulate during the 8–12 h of transport of the air parcel to Riverside.

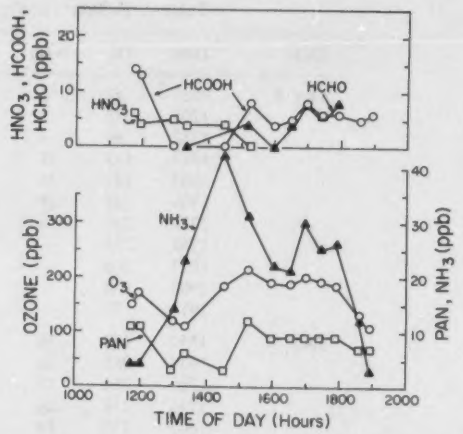

Fig. 10. Time–concentration profiles obtained from 1.08 km pathlength FT-i.r. spectra of Riverside ambient air on October 6, 1976.

Future studies

Modifications to the long-path cell have recently been completed to make it suitable for use as a closed, outdoor 'smog chamber' during the winter months. Specifically, the walls of the cell have been replaced with a tube of 50 μm FEP Teflon film with heat-sealed seams to provide a uniform inert inner surface for the cell. A 1.6 cm i.d. TFE Teflon disperser tube with holes every 0.6 m has been installed along the bottom of the cell to assure good mixing of reactant injections. The initial application of the system in this configuration was a photooxidation study of ppm concentrations of dialkyl amines and oxides of nitrogen under simulated atmospheric conditions (Tuazon *et al.*, 1978). The km pathlength FT-i.r. facility will be returned to ambient air operation for the 1977 summer smog season and primary emphasis will be placed on the further characterization and quantitative determination of various secondary pollutants of importance in the chemistry of the polluted troposphere.

Acknowledgements—The authors gratefully acknowledge the assistance of S. Meinhardt and R. Planck (of SAPRC) and W. Gabbard (of the EPA) in setting up the km pathlength cell. The cooperation and assistance of D. Boen, W. Brown, H. Gillespie and L. Riddle (of UCR) in the siting of this facility on the UCR campus were greatly appreciated. We also wish to thank Dr. D. Grosjean for helpful discussions during preparation of this manuscript. This work was supported by the Environmental Protection Agency (Grant No. 804546-01).

REFERENCES

California Air Resources Board. Effective June 1, 1975 the calibration procedure for ozone was changed from the 2% neutral-buffered potassium iodide method to a u.v. photometry method employing a 1 m u.v. photometer as a primary standard and a Dasibi u.v. ozone analyser as a portable secondary standard for field calibrations (see Pitts *et al.*, 1976).

Chan W. H., Nordstrom R. J., Calvert J. G. and Shaw J. H. (1976) Kinetic study of HONO formation and

decay reactions in gaseous mixtures of HONO, NO, NO_2, H_2O and N_2. *Envir. Sci. Technol.* **10**, 674–682.
Darley E. F., Stephens E. R., Middleton J. T. and Hanst P. L. (1959) Oxidant plant damage from ozone–olefin reactions. *Int. J. Air Pollut.* **1**, 155–163.
Daubendiek R. L. and Calvert J. G. (1975) *Envir. Lett.* **8**, 103–116.
Farber R. J. and Rossano A. T. (1975) A new approach for measuring atmospheric concentrations of ammonia, Air Pollut. Control Ass., Pacific Northwest International Section Meeting, Vancouver, BC, 19–22 Nov.
Finlayson B. J. and Pitts J. N., Jr. (1976) Photochemistry of the polluted troposphere. *Science* **191**, 111–119.
Fitz D. R., Grosjean D. M. and Pitts J. N., Jr. (1976) Unpublished data.
Gay B. W., Jr., Hanst P. L., Bufalini J. J. and Noonan R. C. (1976) Atmospheric oxidation of chlorinated ethylenes. *Envir. Sci. Technol.* **10**, 58–62.
Graham R. A. (1975) The photochemistry of NO_3 and the kinetics of the N_2O_5–O_3 system. Ph.D. Thesis, Chem. Dept., University of California, Berkeley, Calif.
Grosjean D., Doyle G. J., Mischke T. M., Poe M. M., Fitz D. R., Smith J. P. and Pitts J. N., Jr. (1976) The concentration, size distribution, and modes of formation of particulate nitrate, sulfate, and ammonium compounds in the eastern part of the Los Angeles basin. 69th Air Pollut. Control Ass. Annual Meeting, Portland, OR, 27 June–1 July.
Grosjean D. (1977) Chemical transformations, Chap. IV-C. Review prepared for the Subcommittee on Ammonia, National Academy of Sciences, Committee on Medical and Biological Effects of Environmental Pollutants, Washington, DC.
Hanst P. L., Stephens E. R., Scott W. C. and Doerr R. C. (1958) Atmospheric ozone reactions, The Franklin Institute, Philadelphia, Penn.
Hanst P. L. (1971) Spectroscopic methods for air pollution measurement. In *Advances in Environmental Science and Technology* (Edited by Pitts J. N., Jr. and Metcalf R. L.) Vol. 2, pp. 91–213, Wiley-Interscience, New York.
Hanst P. L., Lefohn A. S. and Gay B. W., Jr. (1973) Detection of atmospheric pollutants at parts-per-billion levels by infrared spectroscopy. *Appl. Spectosc.* **27**, 188–198.
Hanst P. L., Wilson W. E., Patterson R. K., Gay B. W., Jr., Chaney L. W. and Burton C. S. (1975a) *A Spectroscopic Study of California Smog*, Environmental Protection Agency, EPA Publication No. 650/4-75-006, Research Triangle Park, N.C.
Hanst P. L., Spiller L. L., Watts D. M., Spence J. W. and Miller M. F. (1975b) Infrared measurement of fluorocarbons, carbon tetrachloride, carbonyl sulfide and other atmospheric trace gases. *J. Air Pollut. Control Ass.* **25**, 1220–1226.
Heuss J. M. and Glasson W. A. (1968) Hydrocarbon reactivity and eye irritation. *Envir. Sci. Technol.* **2**, 1109–1116.
Hirschfeld T. (1976a) Instrumental requirements for absorbance subtraction. *Appl. Spectrosc.* **30**, 550–551.
Hirschfeld T. (1976b) Wavenumber scale shift in Fourier transform infrared spectrometers. *Appl. Spectrosc.* **30**, 549–550.
Kopczynski S. L. and Bufalini J. J. (1971) Some observations on stoichiometry of iodometric analyses of ozone at pH 7.0. *Analyt. Chem.* **43**, 1126–1127.
Mader P. P., Cann G. and Palmer L. (1955) Effects of polluted atmospheres on organic acid composition in plant tissues. *Pl. Physiol.* **30**, 318–323.
McAfee J. M., Winer A. M. and Pitts J. N., Jr. (1974) An infrared product analysis of ozone–olefin reactions by Fourier interferometry, presented at CODATA Symposium on Chemical Kinetics Data for the Lower and Upper Atmosphere, Warrenton, Va; 16–18 Sept.
McAfee J. M., Stephens E. R., Fitz D. and Pitts J. N., Jr. (1976) Infrared absorptivity of the 9.6 micron ozone band as a function of spectral resolution and abundance. *J. quant. Spectrosc. Radiat. Transfer* **16**, 829–837.
McNelis D. N. (1974) Aerosol formation from gas phase reactions of ozone and olefins in the presence of sulfur dioxide. Ph.D. Thesis, University of North Carolina, Chapel Hill, N.C.
Miller D. F. and Spicer C. W. (1974) A continuous analyser for detecting nitric acid. 67th Air Pollut. Control Ass. Annual Meeting, Denver, Col., 9–13 June.
Niki H., Maker P., Savage C. and Breitenbach L. (1975) Fourier transform spectroscopic studies of organic species participating in photochemical smog formation. Int. Conf. Environment Sensing and Assessment, Las Vegas, Nev., 14–19 Sept.
Pitts J. N., Jr., McAfee J. M., Long W. D. and Winer A. M. (1976) Long-path infrared spectroscopic investigation at ambient concentrations of the 2% neutral-buffered potassium iodide method for determination of ozone. *Envir. Sci. Technol.* **10**, 787–793.
Stephens E. R. (1958) Long-path infrared spectroscopy for air pollution research. *Appl. Spectrosc.* **12**, 80–84.
Stephens E. R. (1961) Long-path infrared spectroscopy for air pollution research. *Infrared Physics* **1**, 187–196.
Stephens E. R., Hanst P. L., Doerr R. C. and Scott W. E. (1956a) Reactions of nitrogen dioxide and organic compounds in air. *Ind. Engng Chem.* **48**, 1498–1504.
Stephens E. R., Scott W. E., Hanst P. L. and Doerr R. C. (1956b) Recent developments in the study of the organic chemistry of the atmosphere. *Proc. Am. Petrol. Inst.* **30**, 288; *J. Air Pollut. Control Ass.* **6**, 159–165.
Stephens E. R. and Schuck E. A. (1958) Auto pollution effects of irradiated auto exhaust as related to fuel composition. *Chem. Engng Prog.* **54**, 71–77.
Stephens E. R., Hanst P. L., Doerr R. C. and Scott W. E. (1959) Auto exhaust: composition and photolysis products. *J. Air Pollut. Control Ass.* **8**, 333–335.
Stephens E. R. and Scott W. E. (1962) Relative reactivity of various hydrocarbons in polluted atmospheres. *Proc. Am. Petrol. Inst.* **42** (III), 665–670.
Stephens E. R. and Price M. A. (1973) Analysis of an important air pollutant: peroxyacetyl nitrate. *J. chem. Educ.* **50**, 351–354.
Tuazon E. C., Winer A. M., Schmid J. P., Graham R. A. and Pitts J. N., Jr. (1978) Fourier transform infrared detection of nitramines in irradiated amine–NO_x systems. *Envir. Sci. Technol.* **12** (in press).
White J. U. (1942) Long optical paths of large aperture. *J. opt. Soc. Am.* **32**, 285–288.

Note added in proof: A recent study in our laboratory indicates that the absorptivity for formic acid given in Table 1 is too low. Consequently, the formic acid concentrations reported in this paper should be divided by 2.6.